Thermoelectric power calculation by the Boltzmann equation: Na_xCoO_2

2007 J. Phys.: Condens. Matter 19 365221

(http://iopscience.iop.org/0953-8984/19/36/365221)

IOP PUBLISHING JOURNAL OF PHYSICS: CONDENSED MATTER

J. Phys.: Condens. Matter **19** (2007) 365221 (6pp) doi:10.1088/0953-8984/19/36/365221

Thermoelectric power calculation by the Boltzmann equation: Na_xCoO_2

N Hamada, T Imai and H Funashima

Department of Physics, Tokyo University of Science, 2641 Yamazaki, Noda, Chiba 278-8510, Japan

E-mail: hamada@ph.noda.tus.ac.jp

Received 3 December 2006
Published 24 August 2007
Online at stacks.iop.org/JPhysCM/19/365221

Abstract

A full-potential augmented-plane-wave (FLAPW) band-structure calculation in the local density approximation (LDA) was carried out for hexagonal Na_xCoO_2 ($x = 0.45$, 0.55, 0.66 and 0.75). The Seebeck tensor was estimated by the Boltzmann theory, assuming that the relaxation time is constant on the Fermi surface. The Seebeck tensor is extremely anisotropic; the c-axis Seebeck coefficient varies dramatically with the Na content. The calculation reproduces the experiment semiquantitatively.

1. Introduction

Estimation of the thermoelectric power is receiving much attention from the viewpoint of computational material design (CMD) for thermoelectric equipment to utilize wasted heat and to control the temperature accurately. On the basis of the first-principles band-structure calculation, the Boltzmann equation is applied to estimate the transport coefficient. Applicability of the Boltzmann equation itself and its constant-relaxation-time approximation is, however, questionable for actual materials, and especially for strongly correlated electron systems. In this paper, we examine the applicability to the Na_xCoO_2 system, which is a typical strongly correlated electron system and which has a large Seebeck coefficient [1].

For high-temperature superconductors, it is known that the Boltzmann theory is insufficient, and the many-body theoretical approach is needed to explain the temperature dependences of the transport coefficients [2]. We often experience, however, that the Boltzmann theory can be applied beyond the theoretical limit, and that it gives us valuable information. Experimentally, the temperature dependence of the Seebeck coefficient has a simple metallic behaviour in Na_xCoO_2 if we confine ourselves to the stable hexagonal phase ($x < 0.75$) [3]. The Boltzmann theory may reproduce the temperature dependence and also the magnitude of the Seebeck coefficient.

A full-potential augmented-plane-wave (FLAPW) band-structure calculation in the local density approximation (LDA) was carried out for hexagonal Na_xCoO_2 ($x = 0.45$, 0.55,

0.66 and 0.75). The Seebeck tensor was estimated by using the Kohn–Sham band structure, assuming that the relaxation time is constant on the Fermi surface. We will show that the Seebeck tensor is extremely anisotropic, and that the *c*-axis Seebeck coefficient varies dramatically with the Na content. The calculation semiquantitatively reproduces the experimental result for the Seebeck coefficient. We will discuss the discrepancy between the calculation and the experiment.

In the next section, we briefly show the calculational scheme for the Seebeck coefficient. The result for Na_xCoO_2 is shown in section 3, and concluding remarks are presented in section 4.

2. Evaluation of Seebeck coefficient

We used an all-electron full-potential linearized augmented-plane-wave (FLAPW) method to solve the Kohn–Sham equations selfconsistently. Within the semirelativistic calculation, the potential is local; therefore, the velocity is simply calculated by

$$\boldsymbol{v}_{kn} = \langle \psi_{kn} | \frac{\boldsymbol{p}}{m} | \psi_{kn} \rangle, \tag{1}$$

where $\boldsymbol{p}$ and m are the momentum and the mass of an electron, respectively, and $|\psi_{kn}\rangle$ is the Kohn–Sham eigenstate.

The density of states (DOS) is a standard output in the band structure calculation. The DOS is evaluated by

$$D(\epsilon) = \sum_n \frac{\Omega_c}{(2\pi)^3} \int \frac{\mathrm{d}S_\epsilon}{\hbar |\boldsymbol{v}_{kn}|}, \tag{2}$$

where the integration is performed on the equi-energy surface in the Brillouin zone, and Ω_c is the unit cell volume. The DOS is useful for evaluating and interpreting various physical properties from the electronic band structure. The DOS is, however, not very suitable for considering transport properties, because the DOS does not contain sufficient information on the velocity. A key quantity for the transport property is the 'density of velocity tensor' (DOV) defined by

$$\mathsf{W}(\epsilon) = \sum_n \frac{\Omega_c}{(2\pi)^3} \int \boldsymbol{v}_{kn} \boldsymbol{v}_{kn} \frac{\mathrm{d}S_\epsilon}{\hbar |\boldsymbol{v}_{kn}|}. \tag{3}$$

The energy-surface integration is performed by using a tetrahedron method.

We assume that the relaxation time is constant over the electrons near the chemical potential:

$$\tau_{kn} = \tau (=\text{constant}), \tag{4}$$

and we define two quantities. One is the velocity tensor,

$$\mathsf{M}^{(0)}(T, \mu) = \int \left(-\frac{\partial f_0}{\partial \epsilon} \right) \mathsf{W}(\epsilon)\, \mathrm{d}\epsilon \tag{5}$$

and, the other is an energy-transport tensor,

$$\mathsf{M}^{(1)}(T, \mu) = \int \left(-\frac{\partial f_0}{\partial \epsilon} \right) \mathsf{W}(\epsilon)(\epsilon - \mu)\, \mathrm{d}\epsilon. \tag{6}$$

Then, the electric conductivity, σ, and the Seebeck coefficient, S, are written as

$$\sigma = e^2 \tau \mathsf{M}^{(0)} \tag{7}$$

$$\mathsf{S} = -\frac{1}{eT} \mathsf{M}^{(0)-1} \mathsf{M}^{(1)}. \tag{8}$$

Table 1. Crystal structure of Na_xCoO_2: space group $P6_3/mmc$ (No.194); z is the O position. The Ne–Na atom is a virtual atom with the nuclear charge of $10(1-x)+11x$.

x	a	c	z	
0.45	2.827	10.956	0.0868	
0.55	2.827	10.941	0.0885	
0.66	2.827	10.928	0.0910	
0.75	2.827	10.918	0.0935	
Atom	Site	Position		
Ne–Na	2d	2/3	1/3	1/4
Co	2a	0	0	0
O	4f	1/3	2/3	z

We should note that the Seebeck coefficient, S, is independent of the relaxation time, due to the constant-relaxation-time approximation.

The band structure calculation was performed within the local density approximation (LDA). The analytical form of Vosko, Wilk and Nusair was used for the LDA exchange–correlation energy [4, 5]. The linearization [6] for the APW method was done by the scheme of Takeda and Kübler [7]. The energy cutoff parameters for the plane wave are 8 Hr for the wavefunction and 32 Hr for charge density and the potential. The angular momentum expansion is truncated at $l_{\max} = 7$ for the wavefunction, and at $l_{\max} = 6$ for the charge density and the potential. For layered Na_xCoO_2, the muffin-tin (MT) radii are 2.3 au for Na, 2.0 au for Co, and 1.4 au for O. We take 133 $\boldsymbol{k}$ points in the irreducible Brillouin zone for the hexagonal structure, which corresponds to $12 \times 12 \times 12 = 1728$ $\boldsymbol{k}$ points in the whole zone.

3. Na_xCoO_2

3.1. Crystal structure

The crystal structures used in the band-structure calculations are shown in table 1. The lattice constants are experimental ones [3], while the O position z has been optimized through the total energy calculation for each composition x. The value of $z = 0.0935$ for $x = 0.75$ is in reasonable agreement with the experimental value [8] of $z = 0.0913$ for $x = 0.74$. All the Na atoms are assumed to occupy the 2d site, although some of them may occupy the 2b (0, 0, 1/4) site [8]. Fractional occupation of the 2d site is treated by using a virtual atom (Ne–Na) with the nuclear charge of $10 + x$.

3.2. Band structure

Figure 1 shows the band structure of $Na_{0.66}CoO_2$. We note that the unit cell contains two formula units. The 12 bands below -1.7 eV consist mainly of the O 2p orbitals. The bottom of the 3s band of the Ne–Na virtual atom is seen at 5 eV. A Co atom is surrounded by an O octahedron distorted trigonally. The Co 3d states are split into t_{2g} and e_g states, which produce six bands near the Fermi energy and four bands around 2 eV. The t_{2g} state is further split into a_{1g} and e_g states. Roughly speaking, two a_{1g} bands cross the Fermi level. It is noted that all bands are doubly degenerate on the $k_z = 1/2$ zone-boundary plane due to the spatial and time-reversal symmetries.

Figure 2 shows the hole Fermi surfaces for $x = 0.45$ and 0.66. Since the unit cell contains two equivalent CoO_2 layers, one Fermi surface derived from a CoO_2 layer is cut into two parts.

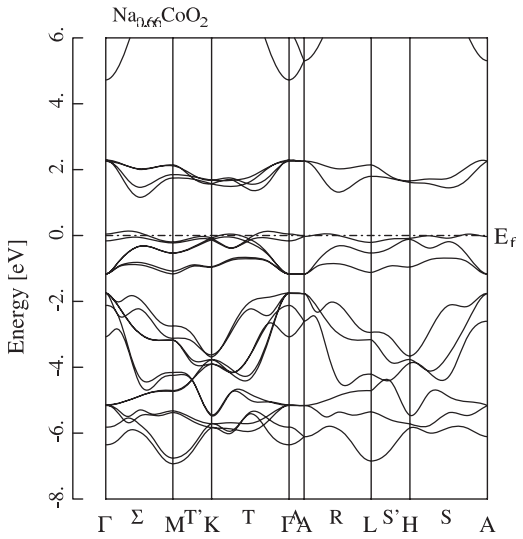

Figure 1. Electronic band structure of $Na_{0.66}CoO_2$ in the virtual-crystal approximation.

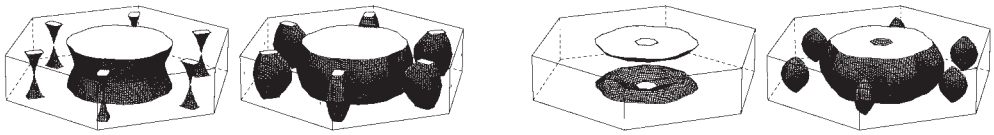

(a) x=0.45 (b) x=0.66

Figure 2. Hole Fermi surfaces for (a) $x = 0.45$ and (b) $x = 0.66$ in Na_xCoO_2.

Table 2. Anisotropy of the velocity tensor, A, at 300 K in Na_xCoO_2.

x	0.45	0.55	0.66	0.75
A	5.9	2.6	1.5	1.1

Those two parts are completely connected on the $k_z = 1/2$ zone-boundary plane due to the symmetry. The Fermi surfaces are two-dimensional at $x = 0.45$, while they become more three-dimensional with increasing x.

Anisotropy of the velocity tensor is defined by

$$A = \frac{\mathsf{M}^{(0)}_{xx} + \mathsf{M}^{(0)}_{yy}}{2\mathsf{M}^{(0)}_{zz}}, \tag{9}$$

which equals the anisotropy of the conductivity within the constant-relaxation-time approximation. Table 2 shows the anisotropy at 300 K for various concentrations. The anisotropy decreases rapidly with increasing the Na concentration x. The large concentration dependence of the anisotropy is an important property of this material.

3.3. Seebeck coefficient

Figure 3 shows the Seebeck coefficients for $x = 0.45$, 0.55, 0.66 and 0.75. In the ab plane, the Seebeck coefficient, $(\mathsf{S}_{xx} + \mathsf{S}_{yy})/2$, increases monotonically with increasing temperature,

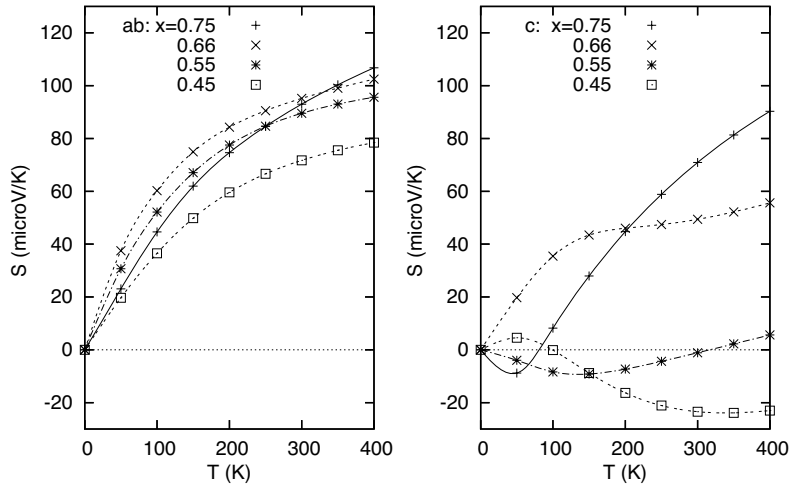

(a) ab-plane (b) c-axis

Figure 3. Seebeck coefficients for $x = 0.45$, 0.55, 0.66, and 0.75 in Na_xCoO_2.

and reaches 90 μV K^{-1} at room temperature for $0.55 \lesssim x \lesssim 0.75$. In the c direction, the Seebeck coefficient, S_{zz}, shows somewhat complex temperature dependence. The behaviour at low temperatures depends on the detail of the band structure near the Fermi surface, which is complicated. At high temperatures, however, the Seebeck coefficient increases monotonically and rapidly with increasing x. For polycrystalline samples, the Seebeck coefficient tends to increase with x [3], which may be attributed to the increase of the c-axis Seebeck coefficient.

4. Discussion and concluding remarks

Our calculation shows that the Seebeck coefficients of Na_xCoO_2 can be explained partially by the Boltzmann theory. There exist some discrepancies between the calculation and experiments. In experiments, Seebeck coefficients larger than 100 μV K^{-1} have been observed at 300 K. For example, Motohashi *et al* [3] observed 120 μV K^{-1} at 300 K for a polycrystalline sample with $x = 0.75$. They also suggested a magnetic order below 22 K by magnetic susceptibility measurement [9]. The magnetic order has been confirmed by using a μSR (muon spin rotation and relaxation) experiment [10]. Such a large Seebeck coefficient may be caused by the spin fluctuation related to the low-temperature magnetic phase.

We have shown the anisotropy of the velocity tensor in table 2. The anisotropy of the electric conductivity is observed to be one order of magnitude larger than the value in this table [1]. This means that the constant-relaxation-time approximation is not applicable for this material. The relaxation time must be at least anisotropic to fit the theoretical conductivity to the experimental value.

Another aspect of the system is randomness in the Na-atom distribution on the 2d and 2b sites. The localization of the electronic states becomes stronger towards the band edge. In general, the Seebeck coefficient becomes larger as the Fermi level approaches the band edge. The extent of localization changes the band edge for mobile electrons (mobility edge). We have to employ a method such as the coherent potential approximation.

The Boltzmann theory is still very much useful if it is carefully applied to the actual material. We also need to develop methods to calculate the many-body theoretical alternatives of τ_{kn} and $\boldsymbol{v}_{kn}$.

Acknowledgment

This work was partially supported by Grant-in-Aids for Scientific Research in Priority Areas 'Development of New Quantum Simulations and Quantum Design' (No. 17064015) of The Ministry of Education, Culture, Sports, Science and Technology, Japan.

References

[1] Terasaki I, Sasago Y and Uchinokura K 1997 *Phys. Rev.* B **56** R12685
[2] Kontani H 2001 *J. Phys. Soc. Japan* **70** 2840
[3] Motohashi T, Naujalis E, Ueda R, Isawa K, Karppinen M and Yamauchi H 2001 *Appl. Phys. Lett.* **79** 1480
[4] Vosko S H, Wilk L and Nusair M 1980 *Can. J. Phys.* **58** 1200
[5] Painter G S 1981 *Phys. Rev.* B **24** 4264
[6] Andersen O K 1975 *Phys. Rev.* B **12** 3060
[7] Takeda T and Kübler J 1979 *J. Phys. F: Met. Phys.* **9** 661
[8] Balsys R J and Davis R L 1996 *Solid State Ion.* **93** 279
[9] Motohashi T, Ueda R, Naujalis E, Tojo T, Terasaki I, Atake T, Karppinen M and Yamauchi H 2003 *Phys. Rev.* B **67** 64406
[10] Sugiyama J, Brewer J H, Ansaldo E J, Itahara H, Tani T, Mikami M, Mori Y, Sasaki T, Hebert S and Maignan A 2004 *Phys. Rev. Lett.* **92** 017602